ISSN 0021-3640, JETP Letters, 2023, Vol. 118, No. 12, pp. 875–880. © The Author(s), 2023. This article is an open access publication.
Russian Text © The Author(s), 2023, published in Pis'ma v Zhurnal Eksperimental'noi i Teoreticheskoi Fiziki, 2023, Vol. 118, No. 12, pp. 871–876.

OPTICS
AND LASER PHYSICS

Efficient Acceleration of Electrons by Moderate-Power Femtosecond Laser Pulses

O. E. Vais[a,b,*], M. G. Lobok[a,b], A. A. Soloviev[c], S. Yu. Mironov[c], E. A. Khazanov[c], and V. Yu. Bychenkov[a,b]

[a] *Lebedev Physical Institute, Russian Academy of Sciences, Moscow, 119991 Russia*
[b] *Center of Fundamental and Applied Research, Dukhov All-Russia Research Institute of Automatics, Moscow, 127030 Russia*
[c] *Federal Research Center Institute of Applied Physics, Russian Academy of Sciences, Nizhny Novgorod, 603950 Russia*
**e-mail: ovais@lebedev.ru*

Received October 13, 2023; revised November 7, 2023; accepted November 9, 2023

The relativistic self-trapping of a laser pulse is an efficient mechanism for the acceleration of electrons, which allows one to achieve an extreme charge of a high-energy particle beam and the corresponding conversion coefficient of laser energy. It has been shown that the compression of the femtosecond laser pulse in this regime using the innovative compression after compressor approach (CafCA) [E.A. Khazanov, S.Yu. Mironov, and G. Mourou, Phys. Usp. **62**, 1096 (2019)] to extremely short durations keeping the energy of the laser beam significantly increases the efficiency of particle acceleration. This effect has been illustrated on the example of the Multitera laser facility for the project implemented at the Russian National Center for Physics and Mathematics.

DOI: 10.1134/S0021364023603548

1. INTRODUCTION

The laser wakefield acceleration in the classical regime of the excitation of a plasma wave [2] or in the so-called bubble regime [3] was the main mechanism of the laser acceleration of electrons for a long time. It allowed one to obtain particle beams with the highest energy and a monochromatic spectrum, which was at the focus of interest [4–6]. At the same time, lower energies of accelerated electrons are sufficient for a number of important problems, but they require much higher total charges of particles that cannot be reached in the wakefield acceleration, which typically provides multipicocoulomb charges [2, 3]. In this case, on the one hand, a laser pulse should stably propagate inside a target to a distance of many Rayleigh lengths, efficiently transferring its energy to accelerated particles and, on the other hand, this target should be dense enough to ensure a much higher total charge of the accelerated electron beam. Both conditions are ensured in the case of the propagation of a relativistically intense laser pulse in the relativistic self-trapping (RST) regime in a plasma with the density up to several tens of percent of the critical density. This regime was identified in [7–10] for ultrarelativistic intense laser pulses with sub-PW and PW powers; in this case, accelerated multi-MeV electron beams had a nanocoulomb charge. However, lasers with such a power do not provide a high pulse repetition rate and a high stability, which are required for most of the applications. For this reason, it is necessary to understand the possibility of implementing the laser acceleration of electrons in the RST regime with much more available femtosecond laser facilities with a much lower power. This problem is solved in this work.

The three-dimensional particle-in-cell simulation [7, 8] shows the possibility of propagation of a relativistically intense laser pulse in a homogeneous plasma with a near-critical density with the formation of a laser–plasma soliton, which is a cavity that is free of electrons, filled with laser light, and moves at a velocity close to the speed of light ("laser bullet," see [11]). The laser bullet stably passes a distance much larger than the Rayleigh length until the loss-induced complete depletion of the laser pulse. Diffraction divergence in this RST regime is balanced by the relativistic nonlinearity of the medium caused by the relativistic increase in the mass of electrons and their cavitation, which leads to the self-consistently establishment of a certain transverse radius of the plasma cavity hardly changes during the entire time of pulse propagation until its depletion. Since this propagation regime is in essence similar to the self-trapping revealed almost 60 years ago for weak stationary laser beams, which are describe by the nonlinear Schrödinger equation with cubic nonlinearity [12–14], it was called the relativistic self-trapping regime [7]. The stationary regime for the laser pulse propagating in the relativistic plasma similar to that found in [12–14] was revealed in [15,

16] by numerically solving the nonlinear Schrödinger equation.

Work [17] supplemented studies [7, 8] with an important case of the RST regime, where the edge at the input of the laser pulse is not sharp but has the form of pre-plasma (density ramp). This situation is experimentally typical, and the possibility of implementing this laser propagation regime in a plasma with an inhomogeneous density profile was proven in [17]. It was shown that the RST regime at the appropriate choice of the position of the focus of the laser pulse with respect to the density profile and the size of the focal spot is as efficient as that in the homogeneous target. This important conclusion allows one to use the homogeneous plasma model in all studies of the considered regime, which is implied below, but refining details can be obtained following [17].

Multi-terawatt laser pulses considered in this work have durations of several tens of femtosecond and can even have a relativistic intensity of interest for RST. However, their power can be additionally increased by the nonlinear decrease in the pulse duration, e.g., using the compression after compressor approach (CafCA) [1, 18, 19]). This approach was based both on the self-modulation of the phase at the propagation of a high-power laser pulse through thin (~1 mm) dielectric plates and on the subsequent correction of the phase of the spectrum due to the reflection of radiation from the surface of chirping mirrors with an anomalous dispersion of group velocities. The self-modulation of the phase broadens the spectrum, and the phase correction ensures the reduction of the duration to a value to the Fourier limit of the pulse with a broadened spectrum. The CafCA allows one to strongly compress the laser pulse and to increase its power without significant changes in the architecture and cost of the laser system. The recent experimental approbation of the CafCA [20–25] has demonstrated the possibility of its efficient application not only in new but also in existing laser systems.

In this work, taking into account the possibility of compression of a laser pulse keeping its energy [26], we aim at showing that the efficiency of the laser acceleration of electrons can be strongly increased using extremely short multiterawatt laser pulses, which is not obvious a priori. This is proven by the three-dimensional PIC simulation of the electron acceleration in the RST regime and opens the important practical possibility of significantly increasing the conversion coefficient to high-energy electrons without an increase in the energy of the laser facility. Below, we give the corresponding illustration on an example of the Multitera laser facility (National Center for Physics and Mathematics).

2. SIMULATION OF THE INTERACTION OF A MULTITERAWATT LASER PULSE WITH A PLASMA TARGET

To analyze the acceleration of electrons in the regime of relativistic self-trapping of a multiterawatt laser pulse, we performed series of three-dimensional PIC simulations of the interaction of the laser beam with plasma targets with various densities using the VSim code (VORPAL, [27]) based on solving the system of Vlasov–Maxwell equations. In these simulations, the laser pulse with a wavelength of 0.8 μm linearly polarized along the z axis propagated along the x axis. The simulations were carried out by the moving window method so that the target where the laser pulse propagates is completely within the computational region. The energy of the laser pulse was 0.85 J, and its duration and the radius of the focal spot were varied (see Table 1). The laser pulse was focused on the boundary of the plasma target, which consists of the fully ionized helium plasma. The assumption of full ionization is justified because the full ionization of the gas in the computational region requires an energy of no more than 10^{-4} of the total energy of the laser pulse. The electron density n_e was chosen such that the focal spot radius of the laser pulse R_L and the characteristic dimensionless field amplitude $a_0 = eE_L/(m_e\omega_L c)$ (where e is the elementary charge, E_L is the characteristic amplitude of the electric field of the laser beam, m_e is the mass of the electron, ω_L is the frequency of laser radiation, and c is the speed of light in vacuum) approximately satisfy the relativistic self-trapping condition

$$R_L \sim \frac{c}{\omega_L}\sqrt{a_0\frac{n_{cr}}{n_e}}, \quad (1)$$

where $n_{cr} = 1.74 \times 10^{21}$ cm^{-3} is the critical density. In the case of relativistically intense laser pulses; i.e., when $a_0 \gg 1$, this condition ensures the stable propagation of a laser–plasma soliton in the target at

Table 1. Total charge $Q_{>20}$, total energy $W_{>20}$, and average energy $\overline{\varepsilon_{>20}}$ of accelerated electrons with energies above 20 MeV and the cutoff energy ε_{max} of the electron spectra obtained for various laser–plasma parameters

τ	40 fs	40 fs	10 fs
R_L	4 μm	2 μm	2 μm
a_0	3.57	7.14	14.3
n_e/n_{cr}	0.006	0.033	0.067
$Q_{>20}$	0.01 nC	2.0 nC	3.1 nC
$W_{>20}$	1 mJ	100 mJ	200 mJ
$\overline{\varepsilon_{>20}}$	130 MeV	55 MeV	70 MeV
ε_{max}	160 MeV	90 MeV	120 MeV

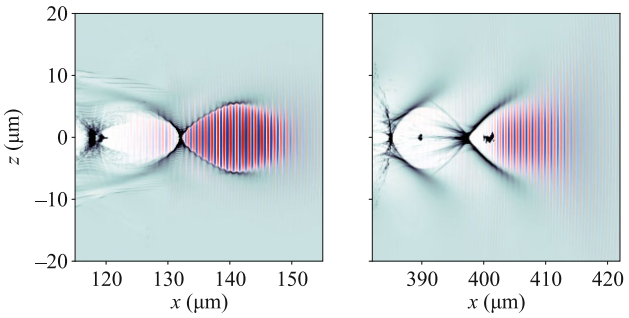

Fig. 1. (Color online) Dynamics of the laser–plasma structure at the propagation of the laser pulse with the duration $\tau = 40$ fs in the low-density plasma target with the electron density $n_e = 0.006n_{cr}$ at the times (left panel) 600 and (right panel) 1500 fs, the electron density distribution in the considered plane is shown in blue–gray, and the E_z component of the laser pulse is given in red–blue. The position of the left edge of the target is $x = 50$ μm.

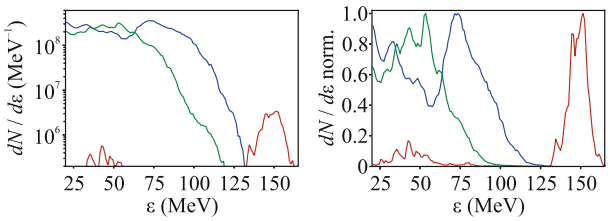

Fig. 2. (Color online) (Left panel) Log–lin and (right panel) lin–lin plots of spectra of electrons accelerated in plasma targets with the electron densities n_e = (red lines) $0.006n_{cr}$, (green lines) $0.033n_{cr}$, and (blue lines) $0.067n_{cr}$ at the propagation of laser pulses with the durations τ = (red and green lines) 40 and (blue lines) 10 fs.

distances much larger than several Rayleigh lengths [9, 10].

The typical durations of laser pulses generated by multiterawatt laser facilities are several tens of femtosecond. For this reason, in the first series of calculations, we considered the interaction of 20-TW 40-fs laser pulses (expected, e.g., from the Multitera laser facility) with targets of various densities. As known, the propagation of a laser pulse through a sufficiently dense plasma, where the plasma wavelength is less than the length of the pulse, $c\tau > \lambda_p$, can be accompanied by the formation of various laser–plasma instabilities such as the filamentation and self-modulation of the laser pulse [28]. To avoid the development of such instabilities, calculations were first performed for a low-density plasma.

In the target with the electron density $0.0015n_{cr}$, the wakefield formation [2] of a three-dimensional plasma wave occurred and the laser pulse was completely inside the first plasma cavity. At such a low electron density, the laser power was only slightly above the critical value for self-focusing and was below the threshold density of the self-injection of electrons, when the acceleration of a noticeable number of particles would require an additional source of electrons [29]. Furthermore, the self-consistent radius of the laser pulse specified by Eq. (1) in such a low-density plasma is large enough (about 6 μm, which corresponds to the half of the length of the laser pulse) and the amplitude a_0 is small, about 1, which is insufficient to reach the RST regime. Some depletion of a low subcritical laser power at a distance of about the Rayleigh length led to the diffraction divergence of laser light at this distance and the laser–plasma structure ceases to exist.

At a higher electron density of $0.006n_{cr}$ in the plasma, the main fraction of the pulse energy was also concentrated in the first plasma cavity, but a small fraction was located in the second plasma cavity (see Fig. 1). In this case, only an insignificant excess of the pulse length over the plasma wavelength did not result in the development of laser–plasma instabilities. The formed laser–plasma structure in the form of a plasma wave with a laser driver changes its form but propagated at distances significantly larger than the Rayleigh length, demonstrating a regime close to the self-trapping of the laser pulse. Moreover, since the considered plasma density was above the electron self-injection threshold, the propagation of the laser pulse inside the target was accompanied by the self-injection of a particle beam with a total charge of 10 pC into the region of the accelerating field of the plasma cavity. Such an electron beam is seen on the right in Fig. 1 inside the first plasma cavity. As a result, the acceleration of particles led to the formation of a quasimonoenergetic spectrum with a maximum at ≈145 MeV (see Fig. 2), and the conversion of the energy of the laser pulse to the energy of accelerated particles was ≈0.1%.

The conversion of the energy of the laser pulse to the energy of accelerated electrons, as well as their total charge, can be increased by a further increase in the plasma density. Correspondingly, we simulated the propagation of the laser pulse in the plasma with a density of $0.033n_{cr}$ with the corresponding decrease in the diameter of the focal spot (see Table 1). In this case, the length of the laser pulse significantly exceeded the plasma wavelength, and the initially formed structure in the form of the plasma channel collapsed behind the laser pulse was separated in the process of propagation in the target in plasma cavities filled with the laser pulse (see Fig. 3). Trailing plasma cavities at the observed self-modulation of the laser pulse were unstable. After the propagation of the laser pulse at a distance of ≈250 μm, which resulted in its significant depletion, the laser–plasma structure was degenerate to a single plasma cavity with remaining laser light in its head part, so-called bubble [3]. In addition, a fraction of the energy of the laser pulse

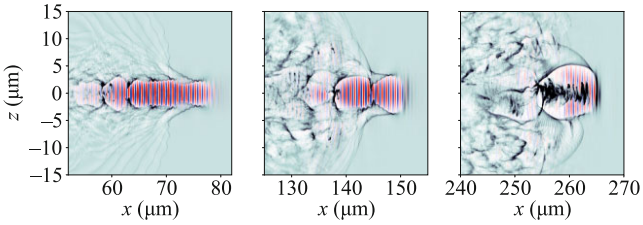

Fig. 3. (Color online) Dynamics of the laser–plasma structure at the propagation of the laser pulse with the duration $\tau = 40$ fs in the plasma target with the electron density $n_e = 0.033n_{cr}$ at the times (left panel) 350, (middle panel) 600, and (right panel) 1000 fs. The position of the left edge of the target is $x = 30$ μm.

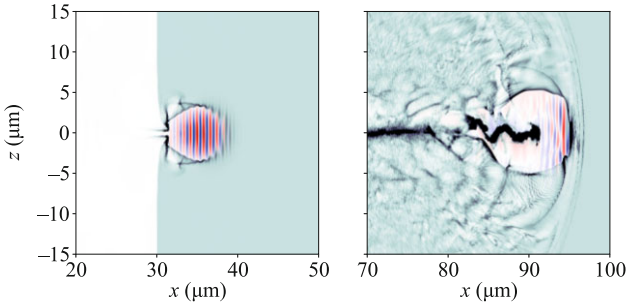

Fig. 4. (Color online) Dynamics of the laser–plasma structure at the propagation of the laser pulse with the duration $\tau = 10$ fs in the plasma target with the electron density $n_e = 0.067n_{cr}$ at the times (left panel) 150 and (right panel) 350 fs. The position of the left edge of the target is $x = 30$ μm.

from trailing cavities was scattered to this time in the transverse direction.

In the last case, the total charge of accelerated electrons with energies above 20 MeV reached a sufficiently high value of ≈2 nC. The spectrum of electrons in a logarithmic scale took a plateau shape and is shown in Fig. 2. Similar plateau spectra were observed for higher-power laser pulses when studying RST in the plasma with a near-critical density in the case of its optimization in the charge of high-energy particles [30]. Furthermore, a similar transition from the monoenergetic spectrum to the plateau shape with increasing plasma density was also discussed in experimental work [31] devoted to laser pulses with energies and durations close to those considered in this work. According to Fig. 2, the cutoff energy of the spectrum ε_{max} determined at a level of 0.1 of the maximum was about 90 MeV, whereas the average energy of particles with energies above 20 MeV was 55 MeV. Thus, the energies of particles were higher in the less dense plasma, but the conversion coefficient of the laser energy in the denser plasma increased to 12% due to an increase in the total charge by two orders of magnitude.

Although the conversion coefficient to high-energy particles increased with the plasma density, instabilities appearing in the process of propagation of a long laser pulse ($c\tau > \lambda_p$) in the plasma resulted in additional losses of its energy. The use of shorter laser pulses, which can be obtained from femtosecond laser facilities applying the CafCA almost without the loss of the laser energy, makes it possible to avoid the development of such instabilities [1]. The authors of [24] have recently shown that this approach allows one to reach durations down to 10 fs, which underlies the below analysis.

We carried out calculations for the 10-fs laser pulse with the same energy as the 40-fs laser pulses considered above. This ensured the increase in the radiation power by a factor of 4 to 80 TW and, as a result, the doubling of the dimensionless field amplitude, which made it possible to use a denser plasma target with an electron density of $0.067n_{cr}$, which satisfies the condition $c\tau \le \lambda_p$. Figure 4 shows the dynamics of the propagation of the formed laser–plasma structure in the form of a solitary plasma cavity. Initially, it was completely filled with the laser pulse and was quasistationary tuned to the self-consistent transverse size. The self-trapping regime in the studied complex dynamic system is manifested as an attractor corresponding to a stable laser–plasma cavity soliton. This attractor attracts the initial states whose parameters approximately satisfy the estimated matching condition (1), which includes the characteristic values of the transverse size of the cavity, plasma density, and laser field, but these parameters vary during the formation of the soliton structure. However, the soliton solution is stable and does not qualitatively change in the process of propagation; only some quantitative changes in the shape of the soliton, in particular, the quasistationary transverse expansion of the cavity by a factor of about 1.5, occurs (see Fig. 4). Such an expansion was already observed in [8, 32]. During the propagation of the laser pulse through the target, a large charge of electrons entered the cavity through its trailing edge and was then accelerated by the transverse field of the cavity. In the reported calculations, the charge of particles accelerated to energies exceeding 20 MeV was ≈3 nC, which is much higher than the value obtained for the 40-fs laser pulse. Moreover, the conversion coefficient of the laser pulse energy to the energy of such particles increased to ≈23.5%, which was accompanied by the increase in both the average and maximum energies of these particles (see Table 1 and Fig. 2). Since energy losses at the conversion of the energy of the laser pulse compressed by the CafCA are insignificant [26], the application of this method will ensure the most efficient generation of high-energy electrons according to the results obtained in this work. Consequently, it is reasonable to carry out the corresponding experiment.

As seen in the calculations, the stable propagation of the laser pulse with a relativistic intensity occurs

under the condition $c\tau \le \lambda_p$, which prevents the development of instabilities, and when the diffraction divergence is compensated by relativistic self-focusing, i.e., under the conditions $a_0 \gg 1$ and (1). In this case, $c\tau \le R$ and $\sqrt{W_L^*/R^2 c\tau} \gg 1$, where $W_L^* = a_0^2 R^2 c\tau$ is the normalized energy of the laser pulse. Therefore, $\sqrt{W_L^*/(c\tau)^3} \gg 1$; i.e., there is the maximum duration at which the RST regime of propagation is possible for a given energy of the laser pulse. The series of numerical simulations showed that this duration for the 0.85-J laser pulse is 40 fs; i.e., the RST regime of propagation without the development of instabilities considered in this work is impossible for longer laser pulses.

3. CONCLUSIONS

To summarize, we have studied the acceleration of electrons accompanying the propagation of a multiterawatt laser pulse in the relativistic self-trapping regime. It has been shown that the maximum duration of a 0.85-J laser pulse that can propagate in the relativistic self-trapping regime without the development of laser–plasma instabilities is 40 fs. The propagation of this laser pulse through a low-density target was accompanied by the formation of a 10-pC electron beam with the conversion coefficient of the laser energy of 0.01%. In a much denser target, the total charge of accelerated electrons and the conversion coefficient increased to 2 nC and 12%, respectively, although laser–plasma instabilities were developed. However, the relativistic self-trapping regime in the dense gas plasma, which is achieved by the compression of the laser pulse, demonstrates the maximum efficiency in terms of the conversion coefficient and the total charge of accelerated particles. For the parameters of the Multitera laser facility, it has been shown that the post-compression of the laser pulse down to 10 fs can ensure the total electron charge and the conversion coefficient of 3 nC and 23%, respectively.

This study has outlined a way to create an efficient laser accelerator of electrons at the Multitera laser facility with the important application of the compression after compressor approach (CafCA), which allows one to significantly extend the applied potential of the laser system.

FUNDING

This study was supported by the National Center for Physics and Mathematics (project "Physics of High Energy Densities. Stage for 2023–2025"). O.E. Vais acknowledges the support of the Foundation for the Advancement of Theoretical Physics and Mathematics BASIS (project no. 22-1-3-28-1).

CONFLICT OF INTEREST

The authors of this work declare that they have no conflicts of interest.

OPEN ACCESS

REFERENCES

1. E. A. Khazanov, S. Yu. Mironov, and G. Mourou, Phys. Usp. **62**, 1096 (2019).
2. T. Tajima and J. M. Dawson, Phys. Rev. Lett. **43**, 267 (1979).
3. A. Pukhov and J. Meyer-ter-Vehn, Appl. Phys. B **74**, 355 (2002).
4. H. T. Kim, K. H. Pae, H. J. Cha, I. J. Kim, T. J. Yu, J. H. Sung, S. K. Lee, T. M. Jeong, and J. Lee, Phys. Rev. Lett. **111**, 165002 (2013).
5. W. P. Leemans, A. J. Gonsalves, H.-S. Mao, K. Nakamura, C. Benedetti, C. B. Schroeder, Cs. Tóth, J. Daniels, D. E. Mittelberger, S. S. Bulanov, J.-L. Vay, C. G. R. Geddes, and E. Esarey, Phys. Rev. Lett. **113**, 245002 (2014).
6. A. J. Gonsalves, K. Nakamura, J. Daniels, et al., Phys. Rev. Lett. **122**, 084801 (2019).
7. V. Yu. Bychenkov, M. G. Lobok, V. F. Kovalev, and A. V. Brantov, Plasma Phys. Control. Fusion **61**, 124004 (2019).
8. M. G. Lobok, A. V. Brantov, and V. Yu. Bychenkov, Phys. Plasmas **26**, 123107 (2019).
9. V. F. Kovalev and V. Yu. Bychenkov, Phys. Rev. E **99**, 043201 (2019).
10. V. Yu. Bychenkov and V. F. Kovalev, Radiophys. Quantum Electron. **63**, 742 (2021).
11. S. V. Bulanov, F. Pegoraro, and A. M. Pukhov, Phys. Rev. Lett. **74**, 710 (1995).
12. V. I. Talanov, Izv. Vyssh. Uchebn. Zaved., Radiofiz. **7**, 564 (1964).
13. R. Y. Chiao, E. Garmire, and C. Townes, Phys. Rev. Lett. **13**, 479 (1964).
14. S. A. Akhmanov, A. P. Sukhorukov, and R. V. Khokhlov, Sov. Phys. JETP **23**, 1025 (1966).
15. A. B. Borisov, A. V. Borovskiy, O. B. Shiryaev, V. V. Korobkin, A. M. Prokhorov, J. C. Solem, T. S. Luk, K. Boyer, and C. K. Rhodes, Phys. Rev. A **45**, 5830 (1992).

16. A. Komashko, S. Musher, S. Turitsyn, et al., JETP Lett. **62**, 860 (1995).
17. V. Yu. Bychenkov and M. G. Lobok, JETP Lett. **114**, 579 (2021).
18. G. Mourou, S. Mironov, E. Khazanov, and A. Sergeev, Eur. Phys. J. Spec. Top. **223**, 1181 (2014).
19. S. Yu. Mironov, S. Fourmaux, P. Lassonde, V. N. Ginzburg, S. Payeur, J.-C. Kieffer, E. A. Khazanov, and G. Mourou, Appl. Phys. Lett. **116**, 241101 (2020).
20. S. Mironov, P. Lassonde, J.-C. Kieffer, E. Khazanov, and G. Mourou, Eur. Phys. J. Spec. Top. **223**, 1175 (2014).
21. Ph. Lassonde, S. Mironov, S. Fourmaux, S. Payeur, E. Khazanov, A. Sergeev, J.-C. Kieffer, and G. Mourou, Laser Phys. Lett. **13**, 075401 (2016).
22. S. Yu. Mironov, V. N. Ginzburg, I. V. Yakovlev, A. A. Kochetkov, A. A. Shaykin, E. A. Khazanov, and G. A. Mourou, Quantum Electron. **47**, 614 (2017).
23. V. Ginzburg, I. Yakovlev, A. Kochetkov, A. Kuzmin, S. Mironov, I. Shaikin, A. Shaykin, and E. Khazanov, Opt. Express **29**, 28297 (2021).
24. A. Shaykin, V. Ginzburg, I. Yakovlev, A. Kochetkov, A. Kuzmin, S. Mironov, I. Shaikin, S. Stukachev, V. Lozhkarev, A. Prokhorov, and E. Khazanov, High Power Laser Sci. Eng. **9**, E54 (2021).
25. A. Soloviev, A. Kotov, M. Martyanov, et al., Opt. Express **30**, 40584 (2022).
26. V. Ginzburg, I. Yakovlev, A. Zuev, A. Korobeynikova, A. Kochetkov, A. Kuzmin, S. Mironov, A. Shaykin, I. Shaikin, E. Khazanov, and G. Mourou, Phys. Rev. A **101**, 013829 (2020).
27. C. Nieter and J. R. Cary, J. Comput. Phys. **196**, 448 (2004).
28. E. Esarey, C. B. Schroeder, and W. P. Leemans, Rev. Mod. Phys. **81**, 1229 (2009).
29. S. P. D. Mangles, G. Genoud, M. S. Bloom, M. Burza, Z. Najmudin, A. Persson, K. Svensson, A. G. R. Thomas, and C.-G. Wahlström, Phys. Rev. ST Accel. Beams **15**, 011302 (2012).
30. M. G. Lobok, A. V. Brantov, D. A. Gozhev, and V. Yu. Bychenkov, Plasma Phys. Control. Fusion **60**, 084010 (2018).
31. J. Faure, Y. Glinec, A. Pukhov, S. Kiselev, S. Gordienko, E. Lefebvre, J.-P. Rousseau, F. Burgy, and V. Malka, Nature (London, U.K.) **431**, 541 (2004).
32. A. Pukhov, S. Gordienko, S. Kiselev, and I. Kostyukov, Plasma Phys. Control. Fusion **46**, B179 (2004).

Translated by R. Tyapaev